photonics

MDPI

Article

Electron Paramagnetic Resonance Sensing of «Hidden» Atomistic and Cooperative Defects in Femtosecond Laser-Inscribed Photoluminescent Encoding Patterns in Diamond

Sergey Vyatkin [1,2,*], Pavel Danilov [1], Nikita Smirnov [1], Daniil Pomazkin [1], Evgeny Kuzmin [1], Alexey Gorevoy [1], Andrey Muratov [1], Ivan Matyaev [3] and Sergey Kudryashov [1,*]

[1] Lebedev Physical Institute, 119991 Moscow, Russia
[2] Geology Faculty, Lomonosov Moscow State University, 119899 Moscow, Russia
[3] Optoelectronic Division, Bauman Moscow State Technical University, 105005 Moscow, Russia
* Correspondence: s.vyatkin@lebedev.ru (S.V.); kudryashovsi@lebedev.ru (S.K.)

Abstract: The changes that appeared in the crystal structure of a natural diamond under the influence of a pulsed femtosecond laser (525 nm) were comprehensively investigated using Fourier-transform infrared (FT-IR), electron paramagnetic resonance (EPR), and photoluminescence (PL) spectroscopy methods. It is shown that changes in the crystal structure occur due to the laser-driven interrelated process of the appearance and migration of interstitial carbon atoms and vacancies. On the one hand, there are atomistic transformations related to a decrease in the concentrations of structural centers that are not associated with vacancies or interstitial atoms—centers A (FT-IR spectroscopy) and P1 and W7 (EPR)—and an increase in the concentration of the H3, NV^0, and NV^- (PL) centers, which are associated with vacancies. On the other hand, there are indications of cooperative effects—an increase in the intensity of multi-atomic B2 (platelets, layers of interstitial carbon atoms (FT-IR)) and N2 (fragments of the structure with broken C–C bonds (EPR)) centers.

Keywords: diamond; femtosecond laser; interstitial carbon atoms; vacancies; paramagnetic centers; atomistic transformations; cooperative effects

Citation: Vyatkin, S.; Danilov, P.; Smirnov, N.; Pomazkin, D.; Kuzmin, E.; Gorevoy, A.; Muratov, A.; Matyaev, I.; Kudryashov, S. Electron Paramagnetic Resonance Sensing of «Hidden» Atomistic and Cooperative Defects in Femtosecond Laser-Inscribed Photoluminescent Encoding Patterns in Diamond. *Photonics* **2023**, *10*, 979. https://doi.org/10.3390/photonics10090979

Received: 10 July 2023
Revised: 24 August 2023
Accepted: 25 August 2023
Published: 28 August 2023

1. Introduction

Diamond, a remarkable crystal with its ultrahigh hardness and broadband (UV–mid IR) electromagnetic transparency, is a well-recognized optical material for scintillators in photoluminescence detectors of high-energy particles [1,2], highly refractive optics [3], single-photon sources [4], and for many other amazing applications. Its unprecedentedly hard lattice robustly keeps high concentrations of different intrinsic (elementary interstitial-vacancy C_i–V pairs, small and large platelets, voidities—defect clusters, dislocations) [5–10] and extrinsic (chemical impurity) defects, considerably affecting its functional—optical, optoelectronic, thermal, and mechanical—characteristics [11]. Irradiation of diamond by high-energy particles—electrons, ions, or neutrons [12,13]—not only brings additional intrinsic defects but could also modify present anchored impurity defects by joining locally generated intrinsic ones [14–16]. Importantly, a multitude of intrinsic and extrinsic defects appears optically active in optical (color centers), IR, or Raman spectroscopy, while another part remains "hidden" and could only be envisioned, e.g., by electron paramagnetic resonance (EPR) spectroscopy [17–20].

Recently, ultrashort-pulse (femtosecond) laser inscription in diamonds emerged as a powerful key-enabling technology for precise and delicate fabrication of color centers in predetermined positions in bulk diamonds for quantum technologies [21], spintronics [22],

and invisible encoding [23]. Mostly, ultrapure IIa-type electronic-grade synthetic diamonds (nitrogen impurity content [N] ~ ppb) were tested by photoluminescence microspectroscopy [21,24,25], revealing the predominant formation of optically active "substitutional nitrogen atom–vacancy" pairs (NV centers) via local laser photoinjection of intrinsic C_i–V pairs [21]. This atomistic transformation was also envisioned via numerical simulations, utilizing different theoretical approaches: density functional theory–molecular dynamics [26], tight binding molecular dynamics [27], and the electron/lattice relaxation model [28]. In diamond samples with higher—ppm-level—concentrations of nitrogen impurities in different aggregation forms, a number of analytical methods—Fourier-transform infrared (FT-IR), optical (UV–near-IR), and photoluminescence (PL) microspectroscopy—were utilized to envision their atomistic transformations, driven by the photoinjected intrinsic defects [23,29]. Moreover, clustering and cooperative processes in the laser-generated microscale dense clouds of intrinsic defects lead to different forms of damage to the diamond lattice, which can be analyzed by the same methods [30–34]. The complementary optical and EPR spectral analysis could shed an informative light on the optically active and optically blind ("hidden") defects resulting from femtosecond laser irradiation.

In this study, FT-IR and PL microspectroscopy methods were accompanied by macroscopic EPR spectral characterization of femtosecond laser-modified regions inside a IaA-type diamond in comparison to its initial non-irradiated structure with a multitude of atomic, diatomic, and cluster impurity centers. This approach made it possible to combine the complementary views of the methods on point- and complex-defect dynamics driven by laser exposure and to investigate for the first time both optically active and optically blind laser-generated defects in diamond.

2. Materials and Methods

The diamond sample was a transparent, flat-faced, octahedral, natural crystal weighing 62 mg (Aykhal pipe, Yakutia, Russia).

Laser exposure of the diamond sample was carried out by a femtosecond laser TEMA (Avesta Project, Moscow, Russia) in 17 separated layers with 96 μm in between in a series of 525 nm, 0.2 ps, 80 MHz, 30 nJ pulses, focused by a 0.25-NA micro-objective (LOMO, St. Petersburg, Russia) into the diamond at the depth of ≈380 μm above the bottom surface. Each layer (2 × 2 mm) consisted of a series of lines with a period of 10 μm written at a speed of 300 μm/s (number of pulses/exposure $N \approx 1.3 \times 10^6$ per point).

IR transmission spectra were obtained using an infrared Fourier-transform (FT-IR) spectrometer, Optics IFS-125HR, with a Hyperion 2000 microscope (Bruker, Billerica, MA, USA).

The photoluminescent (PL) analysis and visualization of the irradiated area were supported by 3D-scanning confocal Raman/PL microspectroscopy (Confotec MR520, SOL Instruments, Minsk, Belarus) with laser excitation at 532 nm and 405 nm.

Electron paramagnetic resonance (EPR) spectra were recorded by an EPR spectrometer, Varian E-115 (Varian, Palo Alto, CA, USA), in X-band (≈9.4 GHz) with a modulation amplitude of 0.1 mT, a modulation frequency of 100 kHz, and a microwave power of 5 mW. The diamond crystal was oriented on the 4-order axes along the vector of the external magnetic field ($H_0 \parallel L4_n$). The concentration of the paramagnetic centers was calculated using an etalon sample.

3. Results and Discussion

As a result of the laser exposure, layers associated with changes in the crystal structure were formed in the diamond under study. Visualization of these layers can be performed using PL microphotography, which is shown in Figure 1.

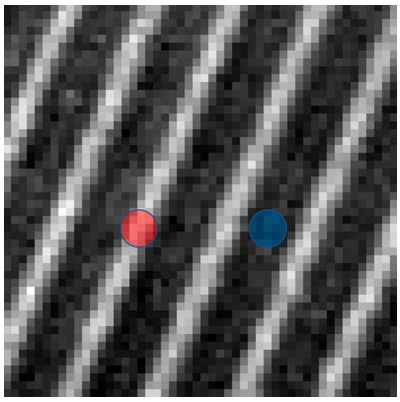

Figure 1. Photoluminescence microphotography (excitation **λ** = 532 nm) of the crystal section after laser exposure. The light areas (marked in red) are the altered layers in the crystal structure of the diamond, the dark areas (blue label) are the unmodified diamond regions. Interlayer distance is 96 μm.

3.1. FT-IR Measurements

The absorption spectra of the diamond sample in the IR range obtained from the areas subjected to laser treatment and not affected by it are shown in Figure 2.

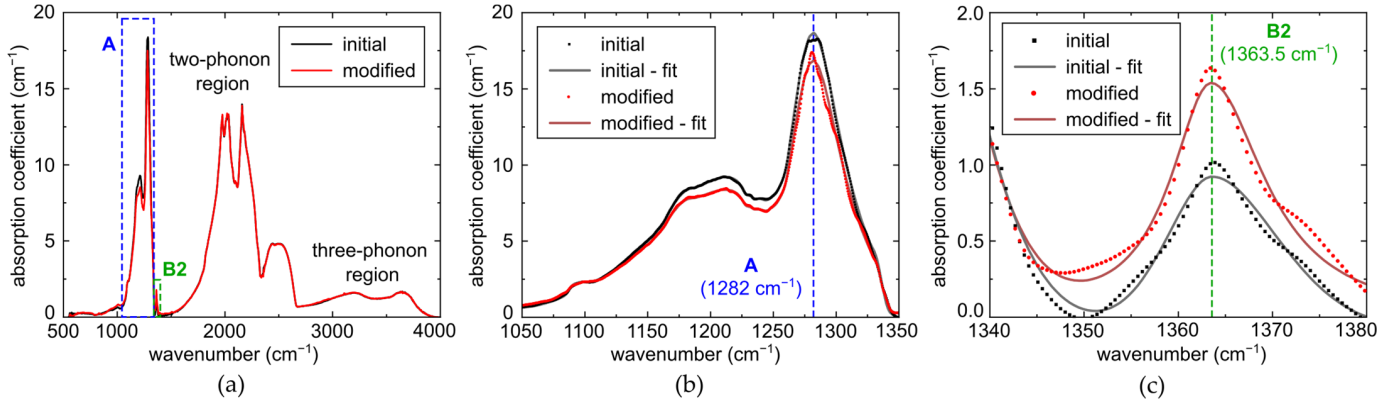

Figure 2. IR absorption spectra of the studied diamond: (**a**) the general view of the spectrum before (black line) and after (red line) laser exposure; (**b**) enlarged part of the spectra with A center peak (1282 cm^{-1}) and B1 center area (1175 cm^{-1}); (**c**) enlarged part of the spectra with B2 peak (1363.5 cm^{-1}) and fitting curves.

The decomposition of the spectrum lines by components in the single-phonon region and the calculation of the concentrations of centers A and B1 (Figure 2b), as well as the fitting of the B2 peak (platelets, Figure 2c), were performed according to [10,35].

The most significant change visible in Figure 2 is a decrease in the intensity of the system of peaks related to the A center. This center represents one of the most common defects in the crystal structure of diamond—two nitrogen atoms replacing carbon in neighboring positions [11]; its main absorption line in the IR spectrum is 1282 cm^{-1}. The decrease in the concentration of the A center for the areas exposed to laser light is more than 13% (from ≈300 ppm to ≈260 ppm). It should be noted that this decrease affects the entire system of absorption peaks related to the A center, including the band around 1215 cm^{-1}. The decrease in the intensity of this band, and not the center line B1 as it may seem at first glance, determines the ratio of the spectra (Figure 2b). The 1175 cm^{-1} line formed by the B1 center (four nitrogen atoms and a vacancy, N_4V) is very low intensity (the calculated concentration of B1 is less than 30 ppm, and it has not changed significantly after the irradiation). The examined diamond sample, therefore, can be attributed to type IaA.

The second important aspect of the changes after laser treatment of the diamond sample, recorded by the FT-IR method, is an increase in the intensity of the 1363.5 cm^{-1} line caused by the B2 center (Figure 2c). The B2 center (or platelets), according to modern concepts [10], is formed by layers of interstitial atoms in the plane <001>. Nitrogen atoms can take part in the formation of B2 centers, but the main part of the platelets consists of interstitial carbon atoms. Due to the variability of the linear dimensions of the platelets, as well as a complex and poorly studied dependence of the absorption intensity in the IR range on their number and size, there is no generally accepted method for recalculating absorption by the number of interstitial atoms in the platelets. In the studied sample, the peak absorption index of B2 centers after the laser exposure increased from 1 cm^{-1} to 1.7 cm^{-1}, while the position of the peak (1363.5 cm^{-1}) and FWHM (12 cm^{-1}) did not change, and the peak area increased from 17 cm^{-2} to 30 cm^{-2}. It can be seen (Figure 2c) that the distribution in the peak region is not unimodal; we can assume the presence of a second peak about 1370 cm^{-1}, which can be interpreted as the presence of groups of platelets of different sizes [9,10]. The diamond sample, according to FT-IR studies, also contains N_3VH centers (peak ≈ 3107 cm^{-1}), but their number is small, and no changes in their concentration have been recorded.

3.2. EPR Measurements

The EPR spectra of the studied diamond crystal are shown in Figure 3, among them those taken before (line A) and after the laser exposure (lines B, C, D). Each of them is a superposition of the spectra of three paramagnetic centers: P1, W7, and N2.

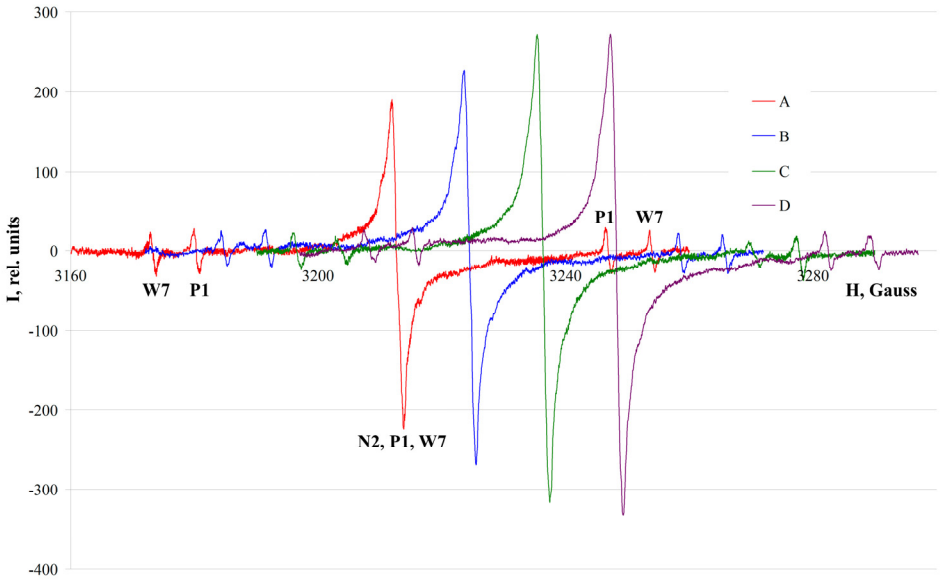

Figure 3. EPR spectra of the studied diamond before (A) and after (B, C, D) laser exposure. The orientation of the crystal was different: spectra A and B were taken with the orientation $H_0 \parallel L4_1$, spectrum C with the orientation $H_0 \parallel L4_2$, spectrum D in the position $H_0 \parallel L4_3$. For clarity, the spectra are shifted relative to each other along the x axis with an interval of 12 gauss. The lines of the paramagnetic centers (P1, W7, N2) are indicated for spectrum A.

The P1 center is a single nitrogen atom replacing carbon in the diamond crystal lattice. The unpaired electron of the nitrogen is localized on one of the four C–N bonds and interacts with the nucleus ^{14}N (I = 1); thus, the axis of symmetry of the hyperfine interaction with ^{14}N is parallel to one of the four (111) bond directions [36]. The calculated concentration of the P1 center for the sample was 0.22 ppm.

The W7 center is formed by two nitrogen atoms replacing carbon at the opposite vertices of a six-membered "ring" in the crystal structure of diamond. These two nitrogen atoms are not equivalent, because the only paramagnetic electron is localized closer to one

of the atoms, which is explained by the loss of one electron after breaking the N–N covalent bond during the transformation of A centers to W7 centers [37]. The content of the W7 centers for the investigated diamond was determined to be 0.81 ppm.

The N2 center causes the appearance of a wide, isotropic single line with a g-factor of 2.003 in the EPR spectrum of diamond; the center does not have an unambiguous structural model. According to [37,38], its paramagnetism is due to broken C–C bonds in the central parts of dislocations; later studies [39] showed that nitrogen is also a part of the center. Finally, in the work [40], a model is put forward that assumes the decoration of deformation dislocations with nitrogen atoms. The initial concentration of the N2 center in the crystal under study was 0.09 ppm. This value was determined by subtracting the contributions of the P1 and W7 centers to the intensity of the central line of the spectrum, which, in turn, were calculated through the intensities of their side lines.

Spectra B, C, and D, shown in Figure 3, reflect the changes that occurred in the crystal after the laser exposure. They were taken under the same conditions as spectrum A, with the orientation of the crystal in three mutually perpendicular directions corresponding to the axes of the 4th order. It should be noted that the intensities of the side lines of the spectrum corresponding to the centers P1 and W7 were slightly reduced after the laser modification. Their concentrations, calculated as the average for a series of measurements, decreased from 0.22 to 0.16 ppm for the P1 center and from 0.81 to 0.72 ppm for the W7 center. It seems quite logical to assume that the contribution of these centers to the intensity of the central line of the spectrum, summed up for the paramagnetic centers identified in the crystal under study, has also decreased. Nevertheless, the intensity of this line, due largely to the N2 center, has increased significantly—from 0.09 to 0.17 ppm. On the one hand, this trend is clearly seen if we analyze the correlation between the intensities of the central and side lines, and on the other hand, the percentage increase in intensity is large enough to exclude its explanation by the influence of possible inaccuracies in the spectrometer settings or sample orientation.

An unexpected result is the uneven distribution of the intensity of the N2 center along different axes of the crystal after the laser irradiation, clearly visible in Figure 3. It should be noted that the anisotropy of some paramagnetic centers (for example, W7), according to structural positions interconnected by cubic symmetry operations, was reported earlier [37]. Such a local decrease in symmetry, that is, the presence of predominant orientations of the paramagnetic center among theoretically equivalent structural positions, was explained by the directional effect during plastic deformation of the crystal. Unlike the paramagnetic center W7, we have not noticed such features for the N2 center before. Their appearance in this experiment may also be explained by the direction of the incident laser light—the orientation of the sample along the largest of the flat faces under the laser exposure.

We support the theory proposed in [40], according to which the N2 center is formed when nitrogen decorates curvilinear deformation dislocations in diamond. The experimentally established presence of preferential orientations of the N2 center relative to the crystallographic axes is already an important fact for clarifying the underlying physical model. Further investigation of this phenomenon can be carried out through experiments on laser modification of diamond from various directions. In this case, the sample must have flat or polished faces perpendicular to different crystallographic directions, as well as a significant initial content of the N2 center.

3.3. PL Measurements

The photoluminescence spectra of the diamond sample acquired before and after the laser exposure are shown in Figure 4.

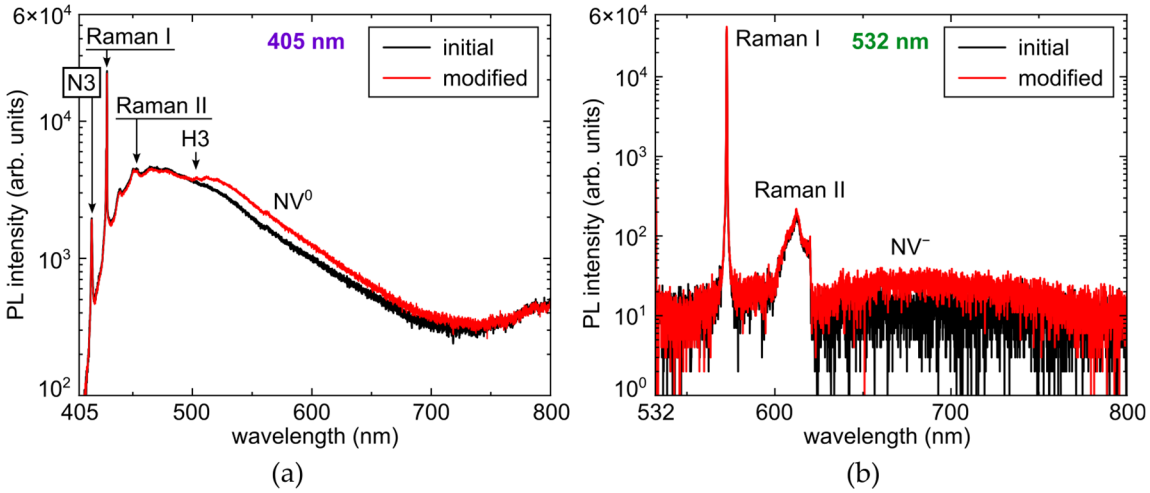

Figure 4. PL spectra of the investigated diamond before and after laser exposure: (**a**) at excitation λ = 405 nm; (**b**) at excitation λ = 532 nm.

After the laser modification of the diamond, the changes registered by the PL method were expressed as an increase in the intensity of the luminescence of H3, NV^0, and NV^- centers. In our previous studies, we investigated the effect of laser exposure time, demonstrating its saturation in Ia and Ib diamonds [33,41].

The H3 center with a zero-phonon line (ZPL) at 503 nm and a phonon band (PB) of 520 nm has a model containing two nitrogen atoms separated by a vacancy [11].

The NV^0 (ZPL 575 nm, PB 600 nm) and NV^- (ZPL 637 nm, PB 680 nm) centers are similar in many ways. Their ZPL accounts for no more than 5% of the total radiation, and the rest is associated with a wide side band. The model of the centers is a nitrogen atom and a vacancy in neighboring positions in the crystal lattice; the difference is only in the charge state of the complex [11].

3.4. Graphitization

Among the changes that intentionally occurred in the diamond crystal under study after the laser exposure, minor undesirable local graphitization was also noted. A few areas of weakly manifested graphitization were found (Figure 5). Typically, they appeared at the intersection of the laser-modified crystal layers and initial cracks. In addition, similar changes were detected as a result of direct laser modification applied to the crystal surface.

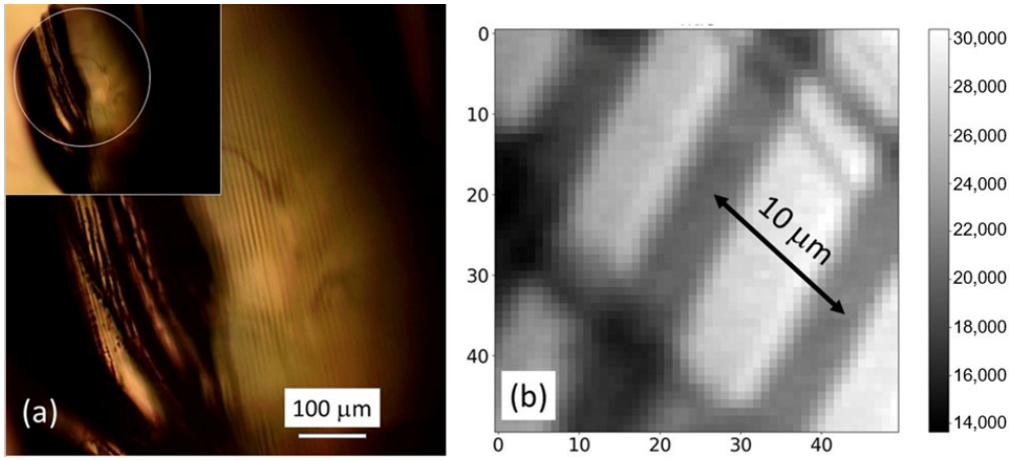

Figure 5. (**a**) Microscope optical image of the diamond with the local graphitized laser tracks (inset—panoramic view) and (**b**) close-view Raman map of the tracks acquired at the Raman peak wavelength 573 nm (excitation wavelength—532 nm).

3.5. Laser-Induced Structural Transformations of Color Centers in the Diamond

According to the results of our spectroscopic study, the analyzed defects in the diamond lattice can be divided into two groups depending on the change in their concentrations after the laser exposure. As indicated in the previous section, on the one hand, the content of the centers A (N–N), P1 (N), and W7 (N–C–C–N) has become smaller. It is noteworthy that all these centers are not associated with vacancies or interstitial atoms. On the other hand, the concentrations of the B2 (platelets, layers of interstitial carbon), N2 (fragments of the structure with broken C–C bonds), and H3 (N–V–N) centers containing vacancies, as well as the NV^0 and NV^- centers, have increased. These findings, in particular, about the conversion of substitutional N atoms into NV centers, are in agreement with the previous experimental [21,24,25,29–31,34] and theoretical [26–28] studies of IIa diamonds, while the diminishing of A center abundance and the rise of H3 center abundance in laser-modified natural diamonds were revealed in [23,32,33]. Meanwhile, laser-driven variation of more complex N2, W7, and B2 centers was observed for the first time and deserves its detailed discussion.

These changes—cooperative effects—are complex and interrelated. Even a simple qualitative examination of changes in the crystal clearly indicates that a decrease in the content of some structural centers and an increase in the concentration of others are the consequences of one process—the formation (and displacement) of interstitial atoms and, accordingly, vacancies. An important remark that needs to be made is the fact that the probability of a nitrogen atom being displaced to the interstitial position is obviously proportional to the total nitrogen content in the crystal, i.e., it is quite small. As a consequence, the nitrogen centers arising in such a process should have a vanishingly low concentration, which cannot be detected by the methods used.

At first glance, the total numbers of the centers of the first and second groups should coincide, but some methodological limitations, e.g., the different volume of the crystal involved in obtaining the spectra using FT-IR, EPR, and PL methods, complicate their quantitative comparison. Moreover, a detailed examination of models describing the centers and their laser-induced modifications in diamond shows that, for almost every concentration-changing center, there are features or alternative schemes of migration of vacancies and interstitial atoms that make quantitative comparison of the initial and resulting content problematic. As an example, we can analyze possible variants of changes in the W7 center registered by the EPR method. It is obvious that the center, whose model is a chain of four atoms (N–C–C–N), has a significant number of variants of changes associated with the transfer of one (or even several) carbon atoms from the composition of the center or from its first coordination sphere to the interstitial position (with the possibility of further migration). There are many potential variants of the resulting modification, which preserve or cause loss to the paramagnetic properties of the center; however, their total content should be taken into account and compared to the drop in the concentration of the initial W7 center equal to 0.09 ppm (as noted in Section 3). Obviously, by means of the research methods used, it is possible to register only those modifications of the W7 center that will contribute to already existing or emerging centers from other sources. Exotic variants of changes in this center, even if they appear, will be unregistered due to very low concentrations. Thus, it can be assumed, for example, that the formation of the NV^0 and NV^- centers from the W7 center is a result of laser exposure; however, their number will be less than the actual decrease in the content of W7 centers. And even the last assumption is ambiguous due to the too close location of nitrogen atoms, with a high degree of probability inherited by any modification of the W7 center.

The exact opposite in terms of the number of possible modifications among the structural disorders under consideration is the P1 center. Due to its simple structure (single substitution of carbon by nitrogen in the lattice), there are practically no alternative options for changing it in the formation of NV^0 and NV^- centers.

As already noted, changes in the crystal structure of diamond as a result of laser exposure are in no way localized around nitrogen atoms. A significant number of vacan-

cies and interstitial carbon atoms occur at significant (in terms of structural parameters) distances from the positions occupied by nitrogen atoms. If we focus on the generation of vacancies, i.e., an increase in the number of sites with broken bonds (C–C) in the crystal structure of the sample, then the most indicative change detected by EPR is, of course, an almost twofold increase in the concentration of the paramagnetic center N2. It should be noted, however, that in the "classical" model of the N2 center, in order to preserve such a configuration, a stabilizing effect of the conditions present in the cores of deformation dislocations is assumed. In the case of the described laser action, it is obvious that bond disturbances in the volume of the crystal lattice are produced randomly and, therefore, may be unstable. From this point of view, it is of interest to estimate the time stability of the changes obtained in the crystal, both under normal conditions and (later) at elevated temperatures, to study possible recombination processes.

The detection of single interstitial carbon atoms (C_i) in the diamond structure is a non-trivial task, requiring very sensitive equipment [19]. However, in our case, the appearance of a significant number of C_i (at least some of them) through the laser generation of C_i–V pairs is recorded as a sharp, almost twofold increase in the absorption of B2 centers (platelets). Since increasing the size (or even the number) of platelets requires not only "building material", in the form of interstitial carbon atoms, but also the possibility of their migration through the crystal, the result obtained allows us to confirm the assumptions made in [19] about the mobility of C_i in the diamond lattice even at room temperature. The B2 centers, as more energetically favorable positions for embedding interstitial carbon than regions of the regular crystal structure, may turn out to be the main C_i concentrators arising during pulsed femtosecond laser action on diamond.

A significant decrease in concentration as a result of the laser exposure, according to the results of experiments, was observed for the A centers (N–N). According to [42], a reduction in their content is interpreted as the capture of a vacancy and a subsequent change in the configuration of the formed center: N–N$-$V $\rightarrow$ H3 (N$-$V$-$N). Regarding the intensity of the photoluminescence of the H3 centers measured in the experiment, it should be noted that at significant concentrations of the A center (the initial content in the studied sample is $\approx$300 ppm), the luminescence of H3 is extinguished due to resonant energy transfer to the nearest A centers [43].

The appearance of insignificant graphitization sites confined to crystal cracks or to its surface, on the one hand, confirms the very possibility of their induction under the influence of a pulsed femtosecond laser in the visible range, reported in [44]. On the other hand, such localization of graphitized areas and their absence in the crystal volume undisturbed by cracks confirm the previously identified value of free oxygen as a catalyst for graphitization processes [45].

4. Conclusions

Exposure of diamond to a pulsed femtosecond laser (525 nm, 0.2 ps, 80 MHz) modifies impurity defects present in the crystal structure due to laser-induced formation of carbon atom vacancies and interstitials. The concentration of defects that are not related to vacancies or interstitials (A, paramagnetic P1, and W7) decreases, while the content of defects that have such a connection (B2, paramagnetic N2, optically active (PL) H3, NV^0, NV^-), on the contrary, increases. A rise in the absorption coefficient of the B2 defect indicates, firstly, the mobility of interstitial carbon under experimental conditions and secondly, the role of platelets as a reservoir of cooperative accumulation (embedding) of emerging interstitials. On the other hand, the formation of carbon vacancies boosts the intensity of the paramagnetic N2 center. Newly formed N2 centers, unlike platelets, may turn out to be unstable, which requires further research on their natural decay and annealing kinetics.

Author Contributions: Conceptualization: S.V. and S.K.; Data curation, A.G.; Formal analysis, A.G.; Funding acquisition, S.K.; Investigation, S.V., P.D., N.S., D.P. and I.M.; Methodology, E.K.; Project administration, S.K.; Supervision, S.K.; Validation, E.K.; Visualization, S.V., P.D., N.S., D.P., A.M. and I.M.; Writing—original draft, S.V., P.D. and S.K.; Writing—review and editing, S.V., A.G. and S.K. All authors have read and agreed to the published version of the manuscript.

Funding: This research was funded by the Russian Science Foundation, grant number 21-79-30063; https://rscf.ru/en/project/21-79-30063/ (accessed on 4 April 2023).

Institutional Review Board Statement: Not applicable.

Informed Consent Statement: Not applicable.

Data Availability Statement: Additional data could be provided by the authors upon a special request.

Conflicts of Interest: The authors declare no conflict of interest.

References

1. Schein, J.; Campbell, K.M.; Prasad, R.R.; Binder, R.; Krishnan, M. Radiation hard diamond laser beam profiler with subnanosecond temporal resolution. *Rev. Sci. Instrum.* **2002**, *73*, 18–22. [CrossRef]
2. Bergonzo, P.; Tromson, D.; Mer, C. Radiation detection devices made from CVD diamond. *Semicond. Sci. Technol.* **2003**, *18*, S105–S112. [CrossRef]
3. Feldman, A. Diamond optics. In *CRC Handbook of Laser Science and Technology Supplement 2*; CRC Press: Boca Raton, FL, USA, 2020; pp. 581–591.
4. Gao, S.; Tian, Z.-N.; Yu, P.; Sun, H.-Y.; Fan, H.; Chen, Q.-D.; Sun, H.-B. Deep diamond single-photon sources prepared by femtosecond laser. *Opt. Lett.* **2021**, *46*, 4386–4389. [PubMed]
5. Humble, P. The structure and mechanism of formation of platelets in natural type Ia diamond. *Proc. R. Soc. Lond. A Math. Phys. Sci.* **1982**, *381*, 65–81.
6. Hirsch, P.B.; Pirouz, P.; Barry, J.C. Platelets, dislocation loops and voidites in diamond. *Proc. R. Soc. Lond. A Math. Phys. Sci.* **1986**, *407*, 239–258.
7. Evans, T.; Kiflawi, I.; Luyten, W.; Tendeloo, G.; Woods, G.S. Conversion of platelets into dislocation loops and voidite formation in type IaB diamonds. *Proc. R. Soc. Lond. Ser. A Math. Phys. Sci.* **1995**, *449*, 295–313.
8. Coomer, B.J.; Goss, J.P.; Jones, R.; Oberg, S.; Briddon, P.R. Identification of the tetra-interstitial in silicon. *J. Phys. Condens. Matter* **2001**, *13*, L1–L7. [CrossRef]
9. Goss, J.P.; Coomer, B.J.; Jones, R.; Fall, C.J.; Briddon, P.R.; Oberg, S. Extended defects in diamond: The interstitial platelet. *Phys. Rev. B* **2003**, *67*, 165208–165215.
10. Speich, L.; Kohn, S.; Wirth, R.; Bulanova, G.; Smith, C. The relationship between platelet size and the B′ infrared peak of natural diamonds revisited. *Lithos* **2017**, *278–281*, 419–426.
11. Ashfold, M.N.R.; Goss, J.P.; Green, B.L.; May, P.W.; Newton, M.E.; Peaker, C.V. Nitrogen in diamond. *Chem. Rev.* **2020**, *120*, 5745–5794.
12. Prawer, S.; Devir, A.D.; Balfour, L.S.; Kalish, R. Infrared emission from selected areas in ion-beam-irradiated diamond. *Appl. Opt.* **1995**, *34*, 636–640. [CrossRef]
13. Green, B.L.; Collins, A.T.; Breeding, C.M. Diamond spectroscopy, defect centers, color, and treatments. *Rev. Mineral. Geochem.* **2022**, *88*, 637–688.
14. Collins, A.T.; Dahwich, A. The production of vacancies in type Ib diamond. *J. Phys. Condens. Matter* **2003**, *15*, L591–L596. [CrossRef]
15. Iakoubovskii, K.; Adriaenssens, G.J.; Dogadkin, N.N.; Shiryaev, A.A. Optical characterization of some irradiation-induced centers in diamond. *Diam. Relat. Mater.* **2001**, *10*, 18–26.
16. Iakoubovskii, K.; Kiflawi, I.; Johnston, K.; Collins, A.; Davies, G.; Stesmans, A. Annealing of vacancies and interstitials in diamond. *Physica B* **2003**, *340–342*, 67–75. [CrossRef]
17. Kirui, J.K.; van Wyk, J.A.; Hoch, M.J.R. ESR studies of the negative divacancy in irradiated type-I diamonds. *Diam. Relat. Mater.* **1999**, *8*, 1569–1571. [CrossRef]
18. Nadolinniy, V.A.; Sobolev, E.V.; Yurieva, O.P. New data on the structure of the R1 and R2 radiation centers in diamond. *J. Struct. Chem.* **1995**, *36*, 626–631. [CrossRef]
19. Twitchen, D.J.; Newton, M.E.; Baker, J.M.; Tucker, O.D.; Anthony, T.R.; Banholzer, W.F. Electron-paramagnetic-resonance measurements on the di-<001>-split interstitial center (R1) in diamond. *Phys. Rev. B* **1996**, *54*, 6988–6998.
20. Twitchen, D.J.; Hunt, D.C.; Smart, V.; Newton, M.E.; Baker, J.M. Correlation between ND1 optical absorption and theconcentration of negative vacancies determined by electron paramagnetic resonance (EPR). *Diam. Relat. Mater.* **1999**, *8*, 1572–1575. [CrossRef]
21. Chen, Y.C.; Salter, P.S.; Knauer, S.; Weng, L.; Frangeskou, A.C.; Stephen, C.J.; Ishmael, S.N.; Dolan, P.R.; Johnson, S.; Green, B.L.; et al. Laser writing of coherent colour centres in diamond. *Nat. Photonics* **2017**, *11*, 77–80.
22. Jelezko, F.; Wrachtrup, J. Focus on diamond-based photonics and spintronics. *New J. Phys.* **2012**, *14*, 105024. [CrossRef]

23. Kudryashov, S.; Danilov, P.; Smirnov, N.; Krasin, G.; Khmelnitskii, R.; Kovalchuk, O.; Kriulina, G.; Martovitskiy, V.; Lednev, V.; Sdvizhenskii, P.; et al. "Stealth Scripts": Ultrashort Pulse Laser Luminescent Microscale Encoding of Bulk Diamonds via Ultrafast Multi-Scale Atomistic Structural Transformations. *Nanomaterials* **2023**, *13*, 192.
24. Chen, Y.C.; Griffiths, B.; Weng, L.; Nicley, S.S.; Ishmael, S.N.; Lekhai, Y.; Johnson, S.; Stephen, C.J.; Green, B.L.; Morley, G.W.; et al. Laser writing of individual nitrogen-vacancy defects in diamond with near-unity yield. *Optica* **2019**, *6*, 662–667. [CrossRef]
25. Yurgens, V.; Zuber, J.A.; Flågan, S.; De Luca, M.; Shields, B.J.; Zardo, I.; Maletinsky, P.; Warburton, R.J.; Jakubczyk, T. Low-charge-noise nitrogen-vacancy centers in diamond created using laser writing with a solid-immersion lens. *ACS Photonics* **2021**, *8*, 1726–1734. [CrossRef]
26. Kempkes, M.; Zier, T.; Singer, K.; Garcia, M.E. Ultrafast nonthermal NV center formation in diamond. *Carbon* **2021**, *174*, 524–530. [CrossRef]
27. Smirnova, M.O. Formation of nitrogen-vacancy centres in diamond: Tight-binding molecular dynamic simulation. *J. Phys. Conf. Ser.* **2020**, *1435*, 012069. [CrossRef]
28. Griffiths, B.; Kirkpatrick, A.; Nicley, S.S.; Patel, R.L.; Zajac, J.M.; Morley, G.W.; Booth, M.J.; Salter, P.S.; Smith, J.M. Microscopic processes during ultrafast laser generation of Frenkel defects in diamond. *Phys. Rev. B* **2021**, *104*, 174303. [CrossRef]
29. Lühmann, T.; Raatz, N.; John, R.; Lesik, M.; Rödiger, J.; Portail, M.; Wildanger, D.; Kleibler, F.; Nordlund, K.; Zaitsev, A.; et al. Screening and engineering of colour centres in diamond. *J. Phys. D Appl. Phys.* **2018**, *51*, 483002. [CrossRef]
30. Kurita, T.; Shimotsuma, Y.; Fujiwara, M.; Fujie, M.; Mizuochi, N.; Shimizu, M.; Miura, K. Direct writing of high-density nitrogen-vacancy centers inside diamond by femtosecond laser irradiation. *Appl. Phys. Lett.* **2021**, *118*, 214001. [CrossRef]
31. Kudryashov, S.I.; Vins, V.G.; Danilov, P.A.; Kuzmin, E.V.; Muratov, A.V.; Kriulina, G.Y.; Chen, J.; Kirichenko, A.N.; Gulina, Y.S.; Ostrikov, S.A.; et al. Permanent optical bleaching in HPHT-diamond via aggregation of C-and NV-centers excited by visible-range femtosecond laser pulses. *Carbon* **2023**, *201*, 399–407. [CrossRef]
32. Kudryashov, S.; Kriulina, G.; Danilov, P.; Kuzmin, E.; Kirichenko, A.; Rodionov, N.; Khmelnitskii, R.; Chen, J.; Rimskaya, E.; Shur, V. Nanoscale Vacancy-Mediated Aggregation, Dissociation, and Splitting of Nitrogen Centers in Natural Diamond Excited by Visible-Range Femtosecond Laser Pulses. *Nanomaterials* **2023**, *13*, 258. [CrossRef]
33. Danilov, P.; Kuzmin, E.; Rimskaya, E.; Chen, J.; Khmelnitskii, R.; Kirichenko, A.; Rodionov, N.; Kudryashov, S. Up/Down-Scaling Photoluminescent Micromarks Written in Diamond by Ultrashort Laser Pulses: Optical Photoluminescent and Structural Raman Imaging. *Micromachines* **2022**, *13*, 1883. [CrossRef] [PubMed]
34. Fujiwara, M.; Inoue, S.; Masuno, S.I.; Fu, H.; Tokita, S.; Hashida, M.; Mizuochi, N. Creation of NV centers over a millimeter-sized region by intense single-shot ultrashort laser irradiation. *APL Photonics* **2023**, *8*, 036108.
35. Speich, L.; Cohn, S.C. QUIDDIT—QUantification of Infrared active Defects in Diamond and Inferred Temperatures. *Comput. Geosci.* **2020**, *144*, 1045–1058. [CrossRef]
36. Loubser, J.; Van Wyk, J.A. Electron spin resonance in the study of diamond. *Rep. Prog. Phys.* **1978**, *41*, 1201–1248. [CrossRef]
37. Shcherbakova, M.Y.; Sobolev, E.V.; Nadolinny, V.A.; Aksenov, V.K. Defects in plastically deformed diamonds by optical and EPR spectra. *Dokl. USSR Acad. Sci.* **1975**, *225*, 566–569. (In Russian)
38. Samsonenko, N.D.; Shulga, V.G.; Litvin, Y.A. Electronic paramagnetic resonance in natural and synthetic diamonds on defects of an unalloyed nature. *Sinteticheskiealmazy* **1970**, *3*, 22–26. (In Russian)
39. Newton, M.E.; Baker, J.M. ^{14}N ENDOR of the N2 center in diamond. *J. Phys. Condens. Matter* **1989**, *1*, 9801–9803. [CrossRef]
40. Mineeva, R.M.; Titkov, S.V.; Speranskii, A.V. Structural defects in natural plastically deformed diamonds according to EPR spectroscopy data. *Geol. Rudn. Mestorozhdenij* **2009**, *51*, 261–271. (In Russian)
41. Kudryashov, S.; Danilov, P.; Kuzmin, E.; Smirnov, N.; Gorevoy, A.; Vins, V.; Pomazkin, D.; Paholchuk, P.; Muratov, A.; Kirichenko, A.; et al. Productivity of Concentration-Dependent Conversion of Substitutional Nitrogen Atoms into Nitrogen-Vacancy Quantum Emitters in Synthetic-Diamond by Ultrashort Laser Pulses. *Micromachines* **2023**, *14*, 1397. [CrossRef]
42. Collins, A.T. A spectroscopic survey of naturally-occurring vacancy-related colour centres in diamond. *J. Phys. D Appl. Phys.* **1982**, *15*, 1431–1438. [CrossRef]
43. Crossfield, M.D.; Davies, G.; Collins, A.T.; Lightowlers, E.C. The role of defect interactions in reducing the decay time of H3 luminescence in diamond. *J. Phys. C Solid State Phys.* **1974**, *7*, 1909–1917. [CrossRef]
44. Kononenko, T.V.; Ralchenko, V.G.; Vlasov, I.I.; Garnov, S.V.; Konov, V.I. Ablation of CVD diamond with nanosecond laser pulses of UV-IR range. *Diam. Relat. Mater.* **1998**, *7*, 1623–1627.
45. Khmelnitsky, R.A.; Gippius, A.A. Transformation of diamond to graphite under heat treatment at low pressure. *Phase Transit.* **2014**, *87*, 175–192. [CrossRef]